Earthquake Scenarios for California Via 3D Physics-based Ground Motion Simulations

Ke Xu[1]; Kim Olsen[2]

[1]North Carolina State University, [2]San Diego State University

Objectives

► Design eight M_w7.0-7.7 **scenario earthquakes** in California each with ensembles of 10 source realizations and simulate the scenarios using 3D physics-based simulations.

► Compare scenario **ShakeMaps** and **PAGER** from simulations and GMMs in terms of estimated MMI, population exposure, and loss probabilities.

Scenario Earthquakes

⇓ **Table 1:** Source descriptions for our eight scenario earthquakes. Top-center locations and 30-year M≥6.7 exceedance probabilities are extracted from UCERF3 (Field et al., 2017), strike, dip, and rake angles are adopted from the SCEC Community Fault Model (CFM) Version 7.0 (Plesch et al., 2024), and along-strike lengths and along-dip widths are estimated by the magnitude-area relationships from Wells and Coppersmith (1994).

Fault (section)	M_w	Top-center loc.	Strike/dip/rake	Length/width (km)	30yr Prob. (M≥6.7)
San Andreas (Peninsula–Loma Prieta)	7.7	(-122.36°, 37.52°) 0 km deep	141°/84°/150°	111/35.2	7.0%
Hayward	7.1	(-122.18°, 37.79°) 0 km deep	328°/74°/180°	67.9/14.4	16.6%
Calaveras	7.1	(-121.43°, 36.93°) 0 km deep	152°/86°/180°	67.9/14.4	16.5%
Concord	7.0	(-122.04°, 37.97°) 0 km deep	161°/86°/180°	58.9/13.5	3.0%
Newport-Inglewood (LA Basin)	7.2	(-118.19°, 33.82°) 0 km deep	317°/79°/180°	78.3/15.3	2.0%
Sierra Madre	7.2	(-118.06°, 34.175°) 0 km deep	296°/59°/60°	57.0/22.0	0.9%
Puente Hills (LA Basin)	7.2	(-118.25°, 33.985°) 5 km deep	293°/27°/90°	57.0/22.0	1.0%
Palos Verdes	7.2	(-118.33°, 33.785°) 0 km deep	124°/19°/120°	57.0/22.0	2.0%

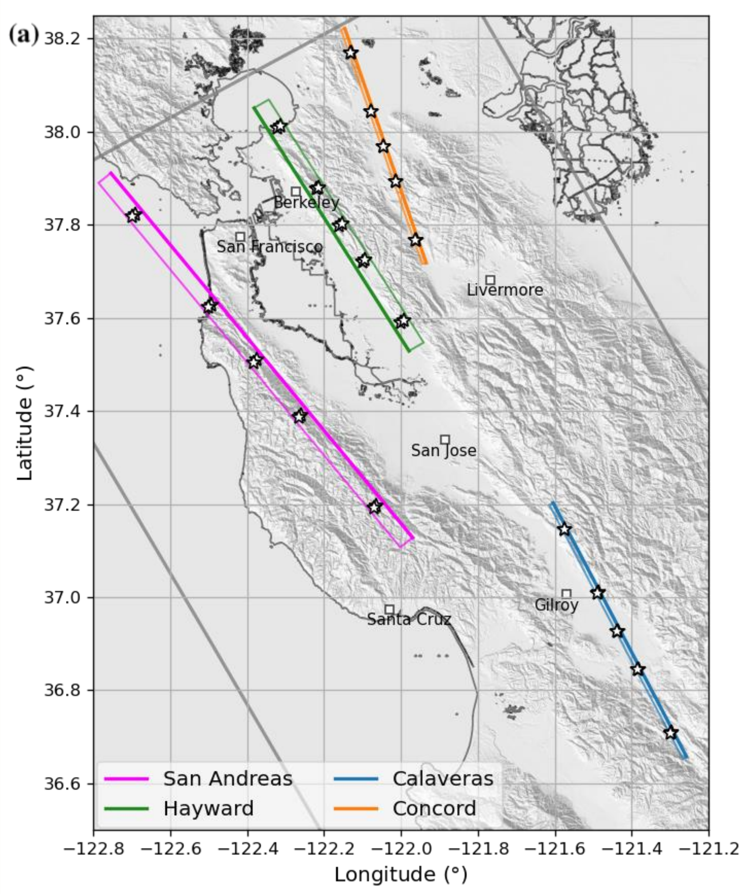

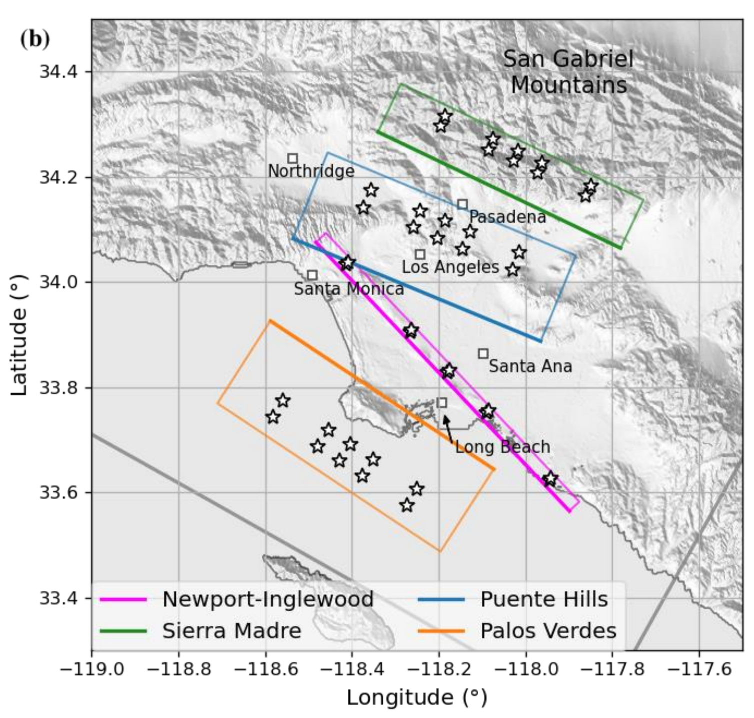

⇑ **Figure 1**: Surface projections of scenario fault ruptures shown as colored boxes and epicenters marked by stars in (a) northern and (b) southern California.

ShakeMap and PAGER from Simulations (continued)

► Higher MMI aligns with the Livermore Basin outside the Bay Area.

► Northern CA scenarios estimate lower exposure (MMI IX+ below 1 million) and losses (zero >1,000 fatality probability) than southern CA;

► Largely due to sparsely and discontinuously distributed population.

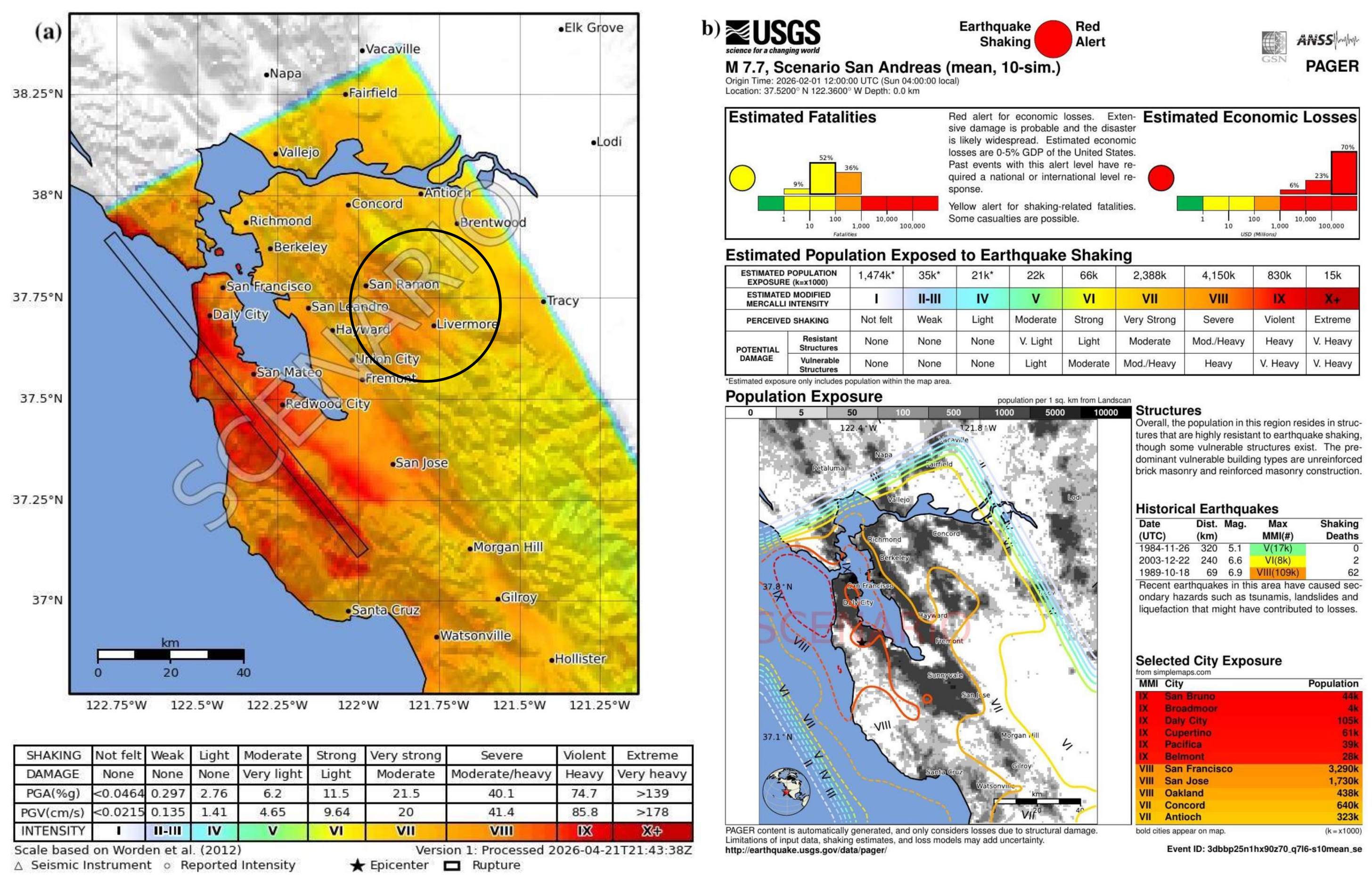

⇑ **Figure 3**: (a) ShakeMap MMIs and (b) PAGER loss estimates from the ensemble mean of a M_w7.7 scenario earthquake on the Northern San Andreas fault.

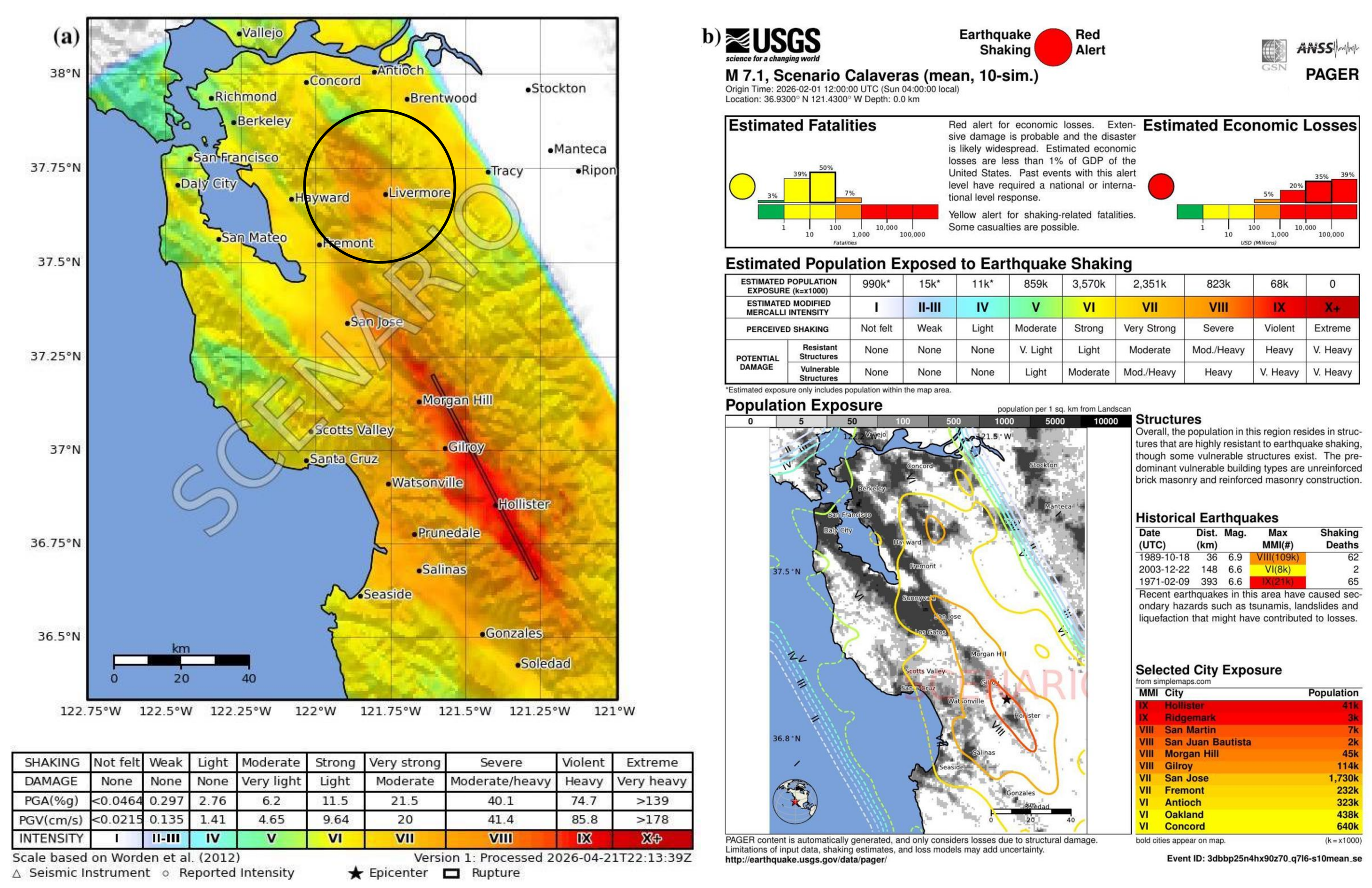

⇑ **Figure 4**: (a) ShakeMap MMIs and (b) PAGER loss estimates from the ensemble mean of a M_w7.1 scenario earthquake on the Calaveras fault.

Comparisons to GMMs (NGA-West2)

► In southern California, the simulations predicts overall higher IMs than the GMMs in basins, aligning closely with the basin–mountain boundaries (Z2.5 surface);

► For the Palos Verdes scenario, the simulations-to-GMM difference is larger at SA-3s, particularly along the northern LA basin edge due to long-period surface waves from the shallow dipping fault and up-dip directivity.

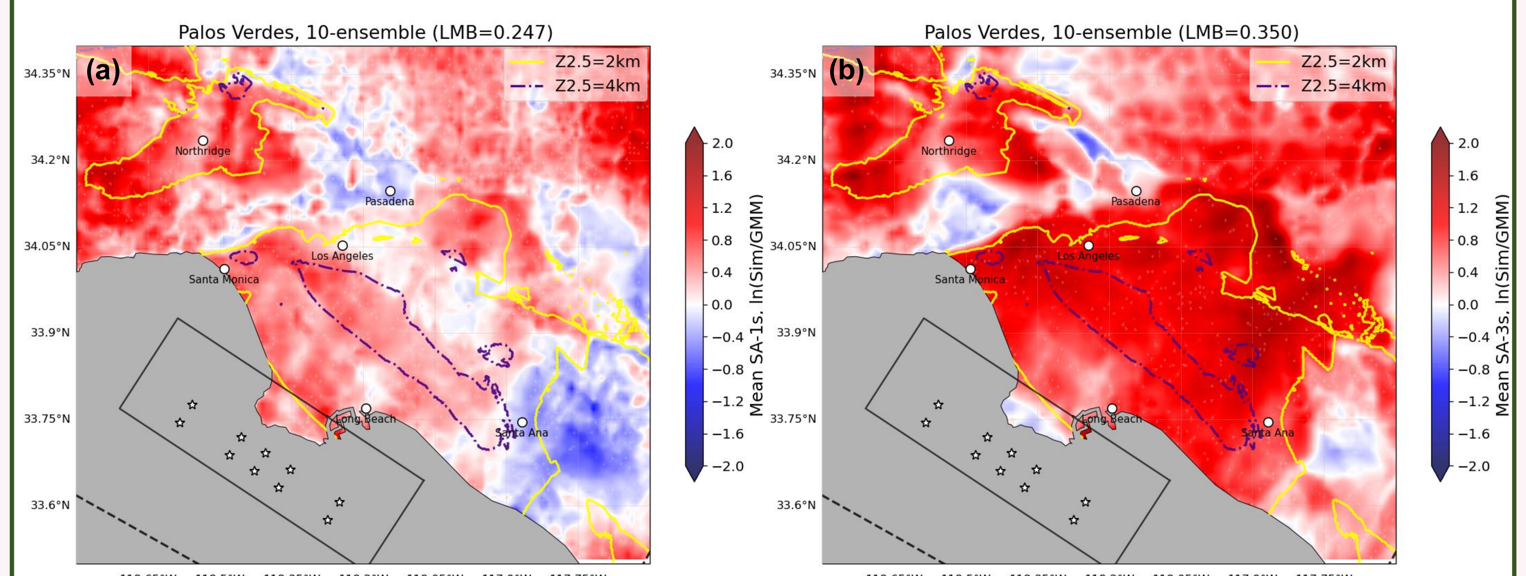

⇑ **Figure 5**: Natural logarithm ratios between IMs generated from the 10-realization ensemble mean 3D simulation and those from GMMs for the M_w7.2 Palos Verdes fault scenario, as (a) SA at 1 s, and (b) SA at 3 s. Background contours show the depth of the Z2.5 surface, while the black box and stars indicate the fault plane and hypocenter locations for the ensemble.

► In northern CA, higher simulation-to-GMM ratios also align with deeper sediments along San Jose - Gilroy and in the Livermore basin;

► Similar or lower IMs compared to the GMMs immediately surround the San Francisco Bay, where the velocity model may need further validations.

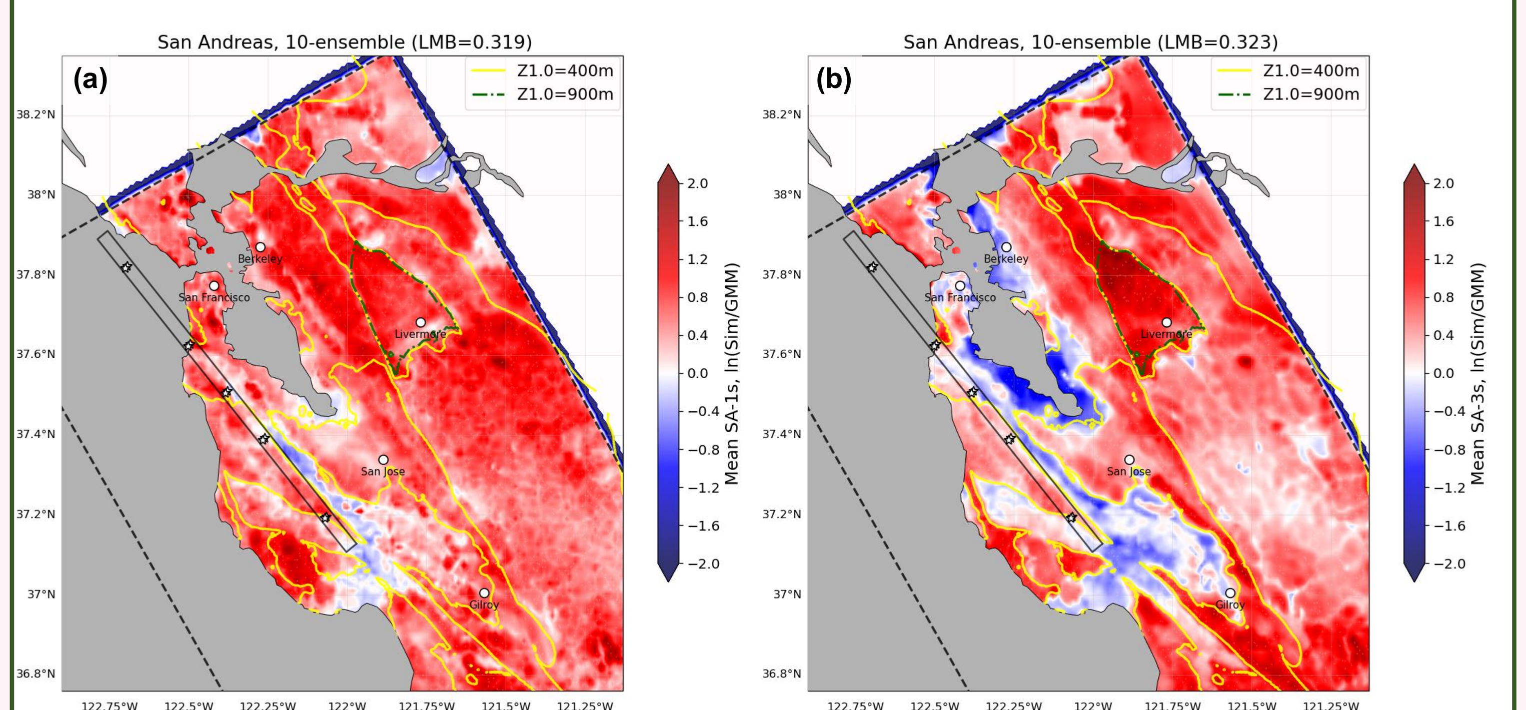

⇑ **Figure 6**: Simulation-to-GMM logarithm ratios for the M_w7.7 Northern San Andreas 10-ensemble fault scenario, as (a) SA at 1 s, and (b) SA at 3 s.

ShakeMap and PAGER from Simulations

► M_w7.2 Newport-Inglewood Fault (Los Angles Basin Section):

- In the ensemble, MMI IX is bounded by the edges of the LA Basin;
- In the southeast-end realization, areas with MMI IX extend into San Fernando basin near Van Nuys, largely due to directivity;
- Ensemble standard deviations up to 45% in terms of SA-3s.
- In PAGER, the ensemble estimates ~5 million people exposed to MMI IX+;
- Southeast-end epicenter realization estimates 2 million higher exposures to MMI IX+ and a 5% higher probability of >1,000 fatalities due to directivity.

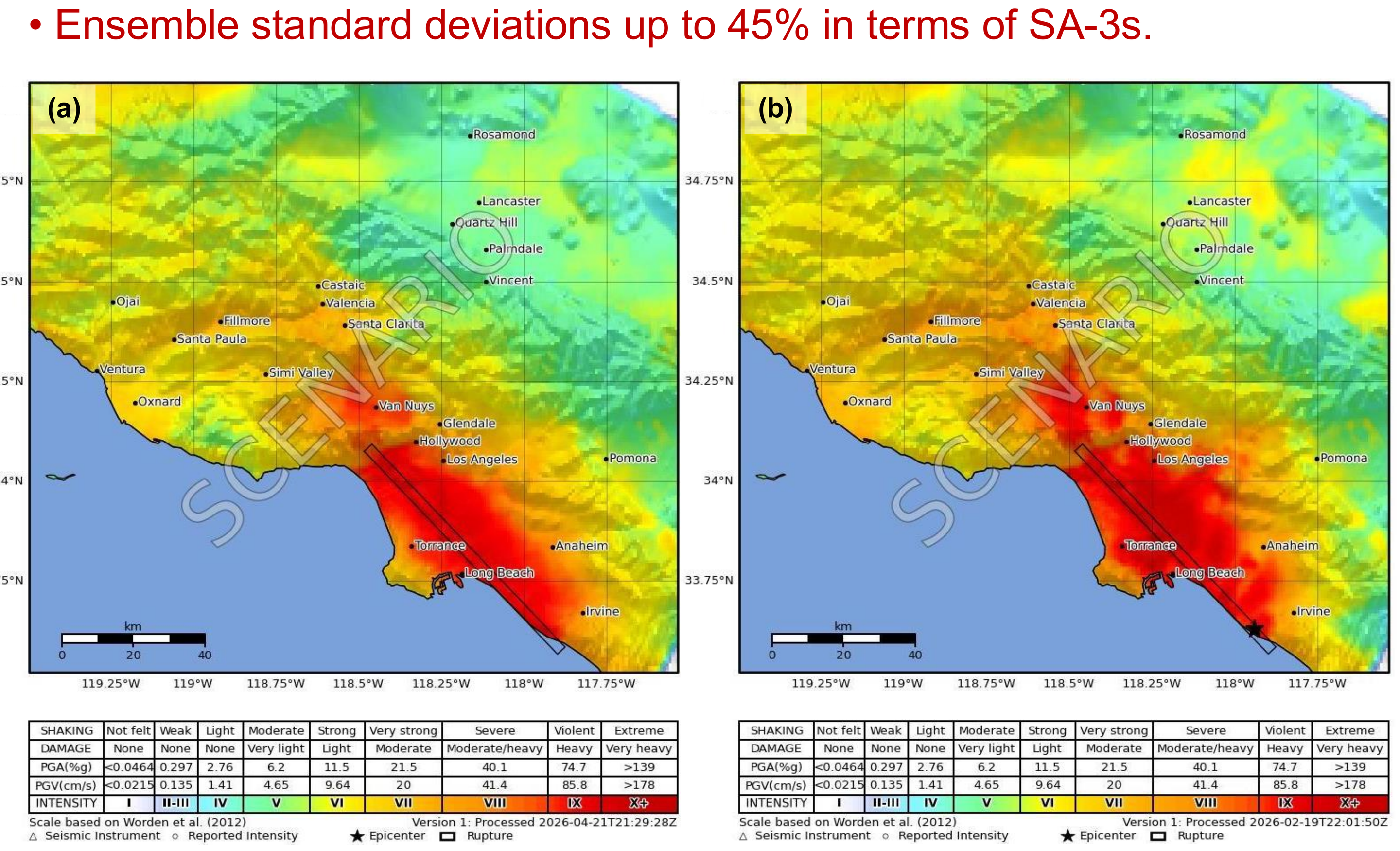

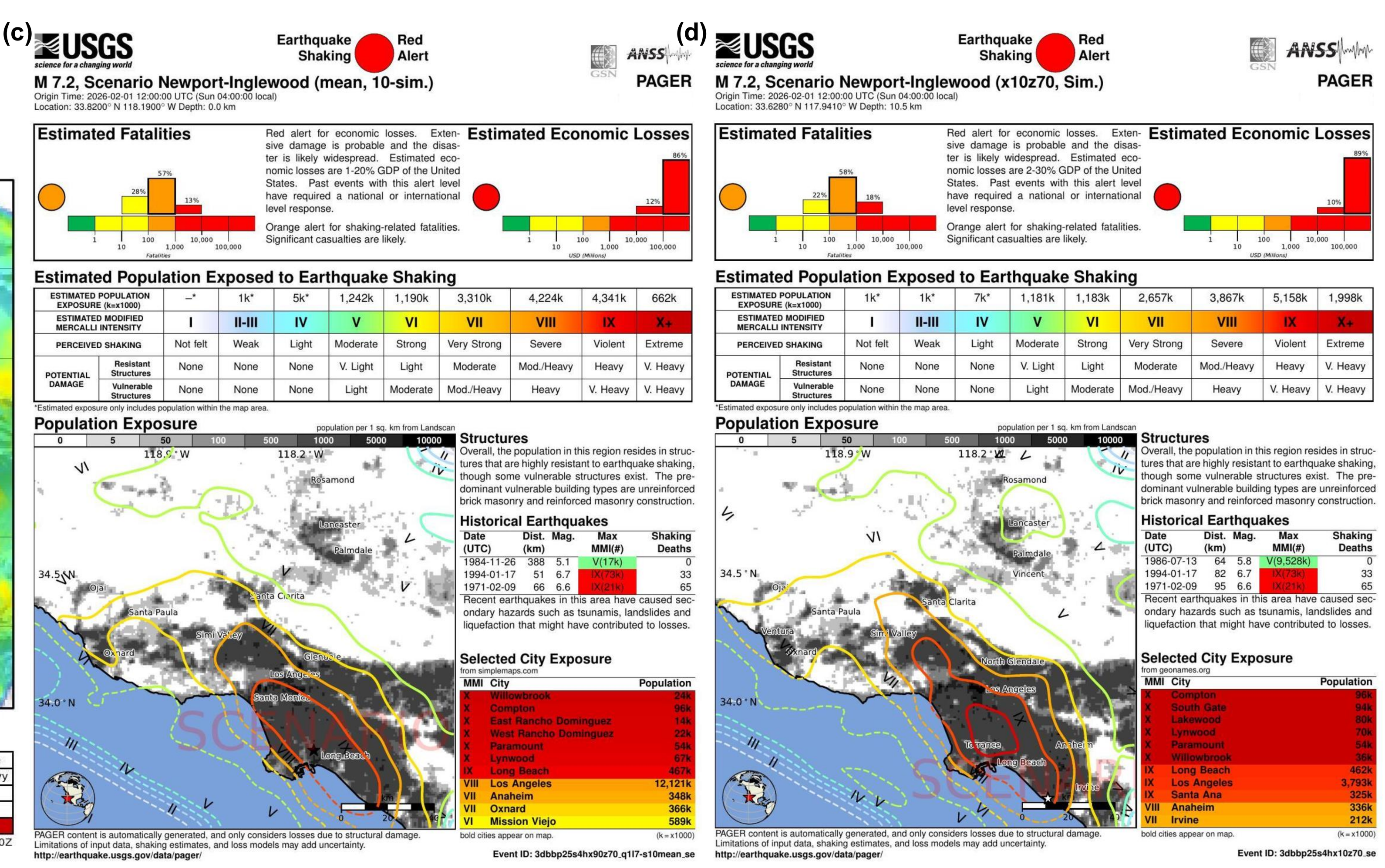

⇑ **Figure 2**: (a-b) ShakeMap MMIs and (c-d) PAGER loss estimates generated from physics-based simulations for a M_w7.2 scenario earthquake on the Newport-Inglewood fault, where (a, c) are from the 10-realization ensemble mean, and (b, d) show a realization with epicenter located near the southeast end of the fault.

Conclusions

► Severe ground motions are predicted in Los Angeles and San Francisco across 10-source-realization ensembles of eight M_w7.0–7.7 scenarios, with intra-ensemble variability reaching ±45%;

► Physics-based simulations predict 80–120% higher IMs than ergodic GMMs in sedimentary basins, largely due to 3D basin and topographic effects;

► Simulations estimate 10–20% higher probabilities of >100 fatalities and larger economic losses, warranting GMM basin corrections be revisited, particularly for the deep southern California basins.

.

References & Acknowledgements

► Field, E. H., T. H. Jordan, M. T. Page, K. R. Milner, B. E. Shaw, T. E. Dawson, G. P. Biasi, T. Parsons, J. L. Hardebeck, A. J. Michael, R. J. Weldon, II, P. M. Powers, K. M. Johnson, Y. Zeng, K. R. Felzer, N. v. d. Elst, C. Madden, R. Arrowsmith, M. J. Werner, and W. R. Thatcher (2017). A Synoptic View of the Third Uniform California Earthquake Rupture Forecast (UCERF3), Seismological Research Letters 88(5), 1259–1267

► Jaiswal, K. and D. Wald (2010). An Empirical Model for Global Earthquake Fatality Estimation, Earthquake Spectra 26(4), 1017–1037.

► O'Reilly, O., T. Yeh, K. B. Olsen, Z. Hu, A. Breuer, D. Roten, and C. A. Goulet (2022). A High-Order Finite-Difference Method on Staggered Curvilinear Grids for Seismic Wave Propagation Applications with Topography, Bulletin of the Seismological Society of America 112(1), 3–22.

► Pitarka, A., R. Graves, K. Irikura, K. Miyakoshi, C. Wu, H. Kawase, A. Rodgers, and D. McCallen (2021). Refinements to the Graves–Pitarka Kinematic Rupture Generator, Including a Dynamically Consistent Slip-Rate Function, Applied to the 2019 Mw 7.1 Ridgecrest Earthquake, Bulletin of the Seismological Society of America 112(1), 287–306.

► Plesch, A., S. Marshall, and J. Shaw (2024). SCEC Community Fault Model (CFM).

► Wald, D. J., C. B. Worden, E. M. Thompson, and M. Hearne (2022). ShakeMap operations, policies, and procedures, Earthquake Spectra 38(1), 756–777.

► Wells, D. L. and K. J. Coppersmith (1994). New empirical relationships among magnitude, rupture length, rupture width, rupture area, and surface displacement, Bull. Seismol. Soc. Am. 84(4), 974–1002.

► We thank Vince Quitoriano and Kishor Jaiswal of the USGS for their guidance and valuable insights regarding ShakeMap and PAGER, and David Wald for his help in generating scenario PAGER products for our study.

► This work was funded by SCEC 2024 award 24156.